Tuning the Electrostatic Interactions in Nanoionic Precipitates for Heavy Metal Ion Detection

IISER PUNE

Sarah Peneena K J

20141039

Under the guidance of

Dr. Pramod P. Pillai

Assistant Professor, Department of Chemistry

Indian Institute of Science Education and Research Pune

Certificate

This is to certify that this dissertation entitled '**Tuning the Electrostatic Interactions in Nanoionic Precipitates for Heavy Metal Ion Detection**' towards the partial fulfillment of the BS-MS dual degree programme at the Indian Institute of Science Education and Research, Pune represents study/work carried out by **Sarah Peneena K J** at **IISER Pune** under the supervision of **Dr. Pramod P. Pillai**, Assistant Professor, Department of Chemistry during the academic year 2018 - 2019.

Signature of Student

Signature of Supervisor

Date: 01/04/2019

Declaration

I hereby declare that the matter embodied in the report entitled 'Tuning the Electrostatic Interactions in Nanoionic Precipitates for Heavy Metal Ion Detection' are the results of the work carried out by me at the Department of Chemistry, IISER Pune, under the supervision of **Dr. Pramod P. Pillai** and the same has not been submitted elsewhere for any other degree.

Signature of Student

Signature of Supervisor

Date: 01/04/2019

Acknowledgement

First and foremost, I would like to convey my sincere gratitude to my research supervisor, **Dr. Pramod P. Pillai**, Assistant Professor, Department of Chemistry, IISER Pune for giving me this wonderful opportunity to carry out my Master's thesis under his guidance. I appreciate his immense knowledge, and especially enthusiasm which helped me to overcome all the difficulties, and stay focused during this short research project. I would also like to thank **Dr. Nirmalya Ballav** for being my TAC member and for his valuable advice and suggestions.

I would like to extend a special recognition to **Anish Rao**. You have stayed with me throughout the ups and downs of my journey, cleared up my mess on many occasions, encouraged me to always have a positive outlook on life, and given me numerous and wonderful suggestions. Despite my shortcomings, thank you for giving me your best!

I am also grateful to all my other lab members. **Soumendu Roy**, I'd like to thank you for helping me with my presentations and writing. I really appreciate your willingness to help me whenever I was in need. **Gayathri Devatha**, conversations have always been enjoyable with you and I'm grateful to you for all the valuable suggestions, care and support that you gave to m. **Sumit Roy**, **Indra Narayan Chakraborty**, **Radhakrishna Kashyap**, it was definitely fun being with you guys, and enjoying each other's nuisances. I thank you all for the constant support and care that you have lent me. In a place far away from home, you guys have been like family to me.

Minal Wable, **Renu Raveendran**, **Vipul Pawar**, **Komal Sah**, **Nivedhika Kannan**, and **Rayan Chakraborty**, you guys have been my closest friends. Your companionship and words of comfort was much needed for me to get through difficult times. Thank you for being there for me.

And finally, I would like to thank each and every staff at IISER Pune for directly or indirectly helping me in finishing this thesis.

Table of Contents

List of Figures

List of Tables

Abstract

The ability to improve and impart new properties in existing nanomaterials is one of the emerging challenges in nanoscience. Our group has recently shown the emergence of selectivity in a traditionally and inherently non-selective carboxylate functionalized gold nanoparticle system ([-] AuNPs). Here, the abilities of different ions were used to break a nanoionic precipitate, where oppositely charged AuNPs are glued together using electrostatic interactions. It was found that the system showed a selective turn on response (appearance of plasmon color) in the presence of Pb^{2+} over other strongly binding divalent ions (M^{2+}). This system, although conceptually attractive, could only detect ~ mM amounts of Pb^{2+} ions. The aim of the present work, described in this thesis is to improve the sensitivity of this system by the mere tuning of interparticle forces. These interparticle forces in question are nothing but the electrostatic interactions which hold together the oppositely charged nanoparticles in the nanoionic precipitate. By weakening the electrostatic interactions, we hypothesize that lesser amounts of Pb^{2+} would be required to break it, thus leading to an improvement in the sensitivity of the detection system. Since the electrostatic interactions are dependent on the ionic strength of the medium and the surface chemistry, they can be used as suitable parameters to control these interactions. In the first part, we study the sensitivity as a function of the ionic strength of the medium. Upon increasing the ionic strength to ~ 300 mM, we observed a ~ 50 fold improvement in the sensitivity of Pb^{2+} detection. Subsequently, by additionally varying the surface chemistry by the use of mixed charge nanoparticle systems, we observed a further improvement (~ 8 fold) in the sensitivity, which is comparable to/ or better than the best known values with carboxylate functionalized nanoparticles. In summary, we were successful in achieving ~ 4μM sensitivity in the detection of Pb^{2+} ions, ***without the aid of any analyte specific ligands.***

Chapter 1: Introduction

Owing to their size confinement in the nanometer regime (1−100 nm), nanomaterials display distinct physical and chemical properties that are not seen when they are present as bulk materials.[1] Consider the case of well-known semiconductors such as CdS, ZnS, GaAs, InP etc. When these materials are confined to nanoscale dimensions (quantum confinement), they display luminescence, which is a property absent in their bulk counterparts.[2] Such materials are called quantum dots.[2] What makes them interesting are their size dependent optoelectronic properties.[2] One can get wide range of colors from the same material by mere variation of the size. Another intriguing example is the case of metal nanoparticles.[3] Unlike the usual lustrous materials that reflect light, their nanomaterial counterparts become strong absorbers (molar absorptivity in the range 10^7 - 10^{11} L mol^{-1} cm^{-1}) of light in the visible range and thus display vibrant colors.[3] The origin of the color is due to a phenomenon termed as Surface Plasmon Resonance (SPR).[3,4] A plasmon is the collective oscillation of free electrons. These oscillations are driven by electromagnetic radiation, and much like the case of a simple harmonic oscillator, the resonance is achieved when the frequency of the radiation matches with the natural frequency of the oscillator.[4] Similar to the case of quantum dots, metal nanoparticles also display different colours based on their size (**Figure 1.1**).[4]

Figure 1.1 Gold nanoparticles of different sizes showing variation in the plasmon color (adapted from reference 5).

There are many other examples of nanomaterials apart from the ones already mentioned, but there is a common thread that connects them all. Apart from the interesting properties they gain on being reduced to such dimensions, what makes them even more attractive are their tunable properties which can be controlled by virtue of size, morphology and surface chemistry.[6,7] Such kind of flexibility is absent at the atomic/molecular and bulk scale. And so, ever since its inception there has been much progress that currently the field is diverging in two different directions. One is the pursuit of new materials with better properties for desired applications and the other focuses on the improvement of properties or imparting newer ones to existing materials.[8] The latter approach is conceptually very challenging since it relies to a large extent on the control of interparticle forces, and thus requires careful design principles. This control on interparticle forces not only improves existing properties, but leads to emergent properties as well. This concept can be best illustrated with an example from the group. Carboxylate nanoparticle systems have been well explored for the trapping of toxic metal ions.[9–13] The metal ions (M^{2+}) bridge the carboxylic groups and lead to the formation of precipitates. But this is an undesired property as it can interfere with the functioning of the system under study. In order to impart improved scavenging properties to this detection system, it was necessary to improve the stability of the M^{2+}–nanoparticle aggregates. Our group devised an ingenious method by which repulsive forces were introduced onto the nanoparticle surface by incorporating a small amount of positively charged ligands ([+]) on the surface of carboxylate functionalized gold nanoparticles ([-] AuNP).[14] By tuning the ratio of [+] and [-], a perfect balance between the attractive and repulsive forces were achieved. This led to the formation of stable M^{2+}–nanoparticle aggregates in the solution, which is an improvement in the existing property of the system. This regulation of interparticle forces also imparted new or emergent properties to the system such as reversibility in the trapping of ions and selectivity between strong (Pb^{2+} and Cd^{2+}) and weak (Ca^{2+}, Mg^{2+}, Na^+ etc.) binding ions.[14] It would be possible to modify this system to further differentiate between the strong binding ions such as Pb^{2+} and Cd^{2+}, but this would not be trivial.

   The major drawback of carboxylate sensors is the absence of selectivity as a result of the strong abilities of M^{2+} ions to bridge carboxylate groups. Due to this non-selective

interaction, the nanoparticles undergo aggregation and plasmon coupling, leading to an immediate colour change, and they subsequently precipitate (turn-off response) in the presence of any M^{2+} ion.[9–13] As a result, they detect both toxic ions (Pb^{2+}, Cd^{2+}) as well as biologically relevant ions (Zn^{2+}, Ca^{2+}, Mg^{2+}).[13] In order to make the AuNPs selective, one has to use analyte specific ligands.[9] Recently, our group showed the emergence of selectivity from a system that is deprived of any analyte specific ligands, which is a conceptually new approach.[15] The system contains oppositely charged AuNPs glued to each other, primarily with electrostatic interactions. The preferential abilities of different strong binding divalent ions to displace [+] AuNPs from the nanoionic precipitates were used as the means of turn-on identification. It was found that out of different ions tested (like Pb^{2+}, Cd^{2+}, Ca^{2+}, Zn^{2+}, Co^{2+}, etc.), only Pb^{2+} could break these electrostatic interactions, and release [+] AuNPs to the solution (turn-on response!). Here, the appearance of wine red color was used as the identification mechanism, as opposed to the disappearance of wine red color (turn-off response). The limit of detection (LOD) for Pb^{2+}, of the [+] – [-] Au nanoionic precipitates was ~ 1 mM, which needs further improvement. The aim of my thesis is to improve the sensitivity of toxic heavy metal ion detection to preferably micro or nanomolar regime, while retaining the selectivity.

  Since the identification mechanism depends on the breaking of electrostatic interactions that hold the [+] – [-] Au nanoionic precipitates together, a decrease in the strength of the electrostatic interactions can demonstrate improvements in the sensitivity of the identification protocol. In this direction, we have employed the following two strategies to regulate the electrostatic interaction holding the nanoionic precipitates together.

Strategy 1:- As electrostatic interactions are dependent on the ionic strength of the medium, we thought of studying the response of [+] – [-] Au nanoionic precipitates with different M^{2+} ions in a medium with high ionic strength (**Figure 1.2**). We chose 50 mM $NaNO_3$ as our working medium. Consequently, the selectivity studies were carried out in the presence of 50 mM $NaNO_3$, and we observed that the sensitivity of the system towards Pb^{2+} improved from ~1.5 mM to 30 μM Pb^{2+} (50 fold improvement in LOD of Pb^{2+} that could be detected with naked eyes). Interestingly, the system still retained selectivity towards Pb^{2+} over Cd^{2+} (40 times more Cd^{2+} was required to visually detect

Cd^{2+} in high ionic strength medium). Systematic studies were undertaken to ascertain the effect of ionic strength on the LOD of Pb^{2+} ions.

Strategy 2:- Next, we discuss an alternative way to tune the electrostatic interactions – by preparing nanoionic precipitates between a homogeneously charged [+] AuNP and heterogeneously charged [+/-] AuNP. Nanoionic precipitates formed from such AuNPs, because of electrostatic repulsions between quaternary ammonium ions, will have lower electrostatic attractions, when compared to [+] − [-] AuNP precipitate. We studied the response of such weakly bound nanoionic precipitates towards M^{2+} ions in solutions of high ionic strengths, which allowed us to accomplish ~ 4μM sensitivity in the detection of Pb^{2+} ions*.*

The present work, therefore, is a step towards our primary aim of introducing the new function of selective as well as sensitive identification of heavy metal ions to nanoparticles by tuning different interparticle interactions, without the use of analyte specific ligands.
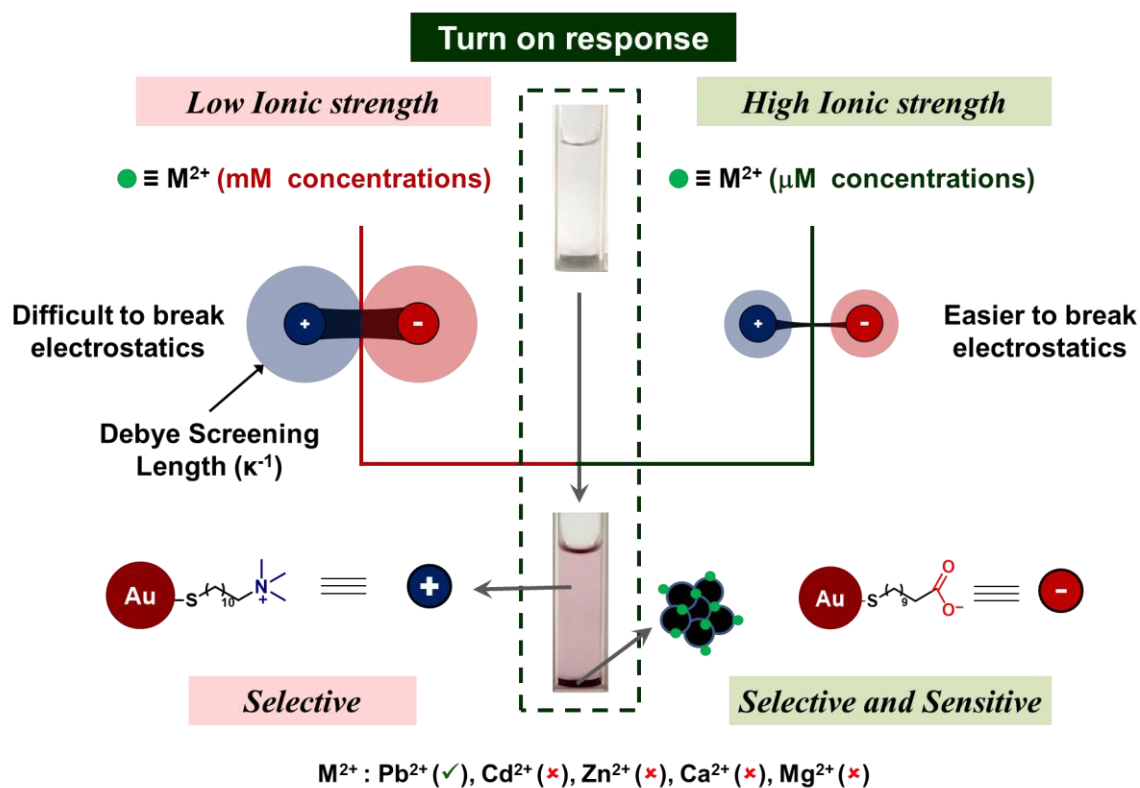

Figure 1.2 Schematics for tuning the sensitivity, as a function of ionic strength, for the identification of heavy metal ions without the use of analyte specific ligands.

Chapter 2: Materials and Methods

2.1 Experimental Section

2.1.1 Materials and Reagents

Tetrachloroaurate trihydrate ($AuCl_4.3H_2O$), Tetrabutylammonium borohydride (TBAB), Hydrazine monohydrate ($N_2H_4.H_2O$, 50-60%), 11-mercaptoundecanoic acid (MUA), Tetramethylammonium hydroxide (TMAOH) 25 % wt. in water, divalent and monovalent salts - $Pb(NO_3)_2$, $Cd(NO_3)_2$, $Zn(NO_3)_2$, $Ca(NO_3)_2$, $Mg(NO_3)_2$, $Ni(NO_3)_2$, $Ba(NO_3)_2$, $NaNO_3$, and KNO_3 were purchased from Sigma Aldrich. (Di-n-dodecyl)dimethyl ammoniumbromide (DDAB) and Dodecylamine (DDA), were purchased from Alfa Aesar. All the reagents were used as received without further purification. All the metal ion stock solutions were prepared in deionized water. The positively charged N,N,N-trimethyl(11- mercaptoundecyl)ammonium ion (TMA) was synthesized according to the reported procedure.[16]

2.1.2 Synthesis of [+], [-], and [+/-]₉ Au NPs (Place Exchange Reaction)

All the nanoparticles were synthesized following a place exchange reaction method. First, Dodecylamine (DDA)- capped Au NPs in toluene were synthesized following a modified reported procedure.[17–19] $HAuCl_4.3H_2O$ was used instead of $AuCl_3$ as the gold precursor, and a mixture of Hydrazine monohydrate ($N_2H_4.H_2O$) and TBAB was used as the reducing agent instead of anhydrous hydrazine. According to this procedure, $HAuCl_4.3H_2O$ (24 mg), DDA (222 mg), and DDAB (277 mg) were taken together in toluene (7 ml) and sonicated for ~10 min to completely solubilize the Au(III) ions. A solution containing a mixture of TBAB (58 mg) and DDAB (111 mg) was rapidly injected to the gold salt solution. The resulting solution (seed solution) was left stirring overnight to ensure the complete reduction of Au(III) ions. The seed particles were then grown to 4.7 ± 0.5 nm DDA-Au NPs. For this, a growth solution was prepared by mixing 1g of DDAB, 2.6 g of DDA, 224 mg of $HAuCl_4.3H_2O$ and 10 ml of seed solution in 60 ml toluene. The growth solution was further reduced with a drop wise addition (in ~30 min) of a 22 mL toluene solution containing 330 µL of $N_2H_4.H_2O$ and 1.2 g of TBAB. The

solution was stirred overnight for the complete growth of the particles yielding monodisperse 4.7 ± 0.5 nm of DDA-Au NPs.

2.1.3 Place Exchange of AuNPs

The Au-DDA NPs (20 mL) were purified using 50 mL methanol yielding a black precipitate, which was then redispersed in 20 mL toluene after decanting the supernatant. Place exchange was initiated by adding a solution of ~ 40 fold molar excess ligand (either [+] or [-]) in 10 mL dichloromethane (DCM) to the toluene solution, and left overnight to ensure complete place exchange. Next, the supernatant was discarded by decantation, and the precipitate was washed with DCM (3 x 50 mL) and finally with acetone (50 mL). The precipitate was then dried, and redispersed in water by adding 20 µL of TMAOH. In the case of [+/-]$_9$ AuNP, a mixture of the ligands was taken in the ratio, [+] : [-] = 1 : 9 for place exchange.

2.1.4 Synthesis of [+] - [-] Au Nanoionic Precipitates

The nanoionic precipitates were synthesized according to previous reports.[20] Stock solutions of similar sized [+] and [-] AuNPs were used. According to the procedure, a solution of [+] AuNP in 3 mL deionized water (~ 6 nM in terms of AuNPs) was titrated with aliquots (~ 0.07 equivalents) of [-] AuNP. After each addition, a period of 15 minutes was given for equilibration and the absorbance was recorded in a UV-Vis spectrophotometer. The additions were continued till AuNPs precipitated from the solution, which corresponded to ~ 6 nM [-] AuNP (electroneutrality condition: nanoionic behavior). A similar procedure was adopted for the synthesis of [+] - [+/-]$_9$ Au nanoionic precipitates. In this case, ~ 6 nM [+/-]$_9$ AuNP was titrated with aliquots (~ 0.07 equivalents) of [+] AuNP. The sharp precipitation occurred on addition of ~ 4 nM [+] AuNPs.

2.1.5 Titration of Au Nanoionic Precipitates with Various M^{2+} Ions

We first carried out M^{2+} binding experiments with [+] - [-] AuNP precipitates (Au nanoionic precipitates) in water (3 mL), which was already reported by our group.[15] The purpose here was to reproduce and validate the reported experimental conditions, so as to follow the same protocol to prove the objective of the present work. In a typical

experiment, small aliquots (3 - 20 µL) of M^{2+} were added to the [+] - [-] Au nanoionic precipitates, and the absorption spectrum of the [+] AuNP released into the solution was recorded. The additions were continued till the plasmon intensity of the [+] AuNP released into the solution got saturated. The limit of detection (LOD) corresponds to the concentration of M^{2+} which gives the minimum colour change visible to the naked eye (corresponds to an optical density of ~ 0.05). The maximum revival corresponds to the concentration of M^{2+} above which no increase in plasmon intensity was observed. To study the behavior of [+] - [-] Au nanoionic precipitates in media of higher ionic strength, a similar approach was adopted. The only point of difference is that after the synthesis of the nanoionic precipitates in water, the supernatant was replaced by adding 3 mL of $NaNO_3$ or KNO_3 solution of the desired concentration. In the case of [+] - [+/-]$_9$ Au nanoionic precipitates, the studies were undertaken in media of higher ionic strength following a similar procedure as in the case of [+] - [-] Au nanoionic precipitates.

2.2 Instrumentation

2.2.1 UV-Vis Studies

The UV-Vis spectra were recorded in a Shimadzu UV-3600 spectrophotometer in an optical glass cuvette (10 mm path length) over the range of 400-800 nm. The concentration of the nanoparticles was taken such that the optical density was ~0.32 (~ 6 nM in terms of AuNPs). The pH of the nanoparticles solution was ~7.

2.2.2 Zeta Potential (ζ) Studies

The zeta potential was measured using a Nano ZS90 (Malvern) Zetasizer instrument. The optical density of the nanoparticle solutions was kept around ~0.3. The zeta potential was determined by measuring the electrophoretic mobility and by use of Henry's equation,

$$U_E = \frac{2\varepsilon z f(\kappa_a)}{3\eta}$$

Where,

U_E is the electrophoretic mobility

z is the zeta potential

ε is the dielectric constant

η is the viscosity

$f(\kappa_a)$ is Henry's function

The zeta potential was derived from the electrophoretic mobility by using Smoluchowski's approximation. The zeta potential values reported were based on an average of five measurements, and the error was less than 2 mV in all the nanoparticle systems.

2.2.3 Transmission Electron Microscopy

The High Resolution Transmission Electron Microscopy (HRTEM) was carried out using a JEOL JEM-2200FS Field Emission Microscope at 200 keV. The samples were diluted and drop cast on a 400 mesh carbon coated copper grid (Ted Pella Inc.) and kept under vacuum. The samples were prepared such that the drying effect was minimum. For this, a drop of the sample was drop casted onto the grid, and after a short time of ~10 minutes, the solvent was removed using a tissue paper.

2.2.4 Scanning Electron Microscopy

The Field Emission Scanning Electron Microscopy was performed using a Zeiss ULTRA PLUS model (0 - 30 keV). The samples were drop cast onto a clean silicon wafer, and dried under vacuum. Care was taken to minimize the drying effect during sample preparation.

Chapter 3: Results and Discussion

3.1 Synthesis of [+] and [-] AuNP

Oppositely charged AuNPs were synthesized by undertaking a place exchange protocol on DDA capped AuNPs (**Figure 3.1.(a)**).[18] N,N,N-trimethylmercaptoundecyl ammonium chloride (TMA, [+]) and 11-mercaptoundecanoic acid (MUA, [-]) were used to obtain positive and negative surface charges on the AuNPs, respectively. The prepared AuNPs were well characterized with UV-Vis. absorption, Transmission Electron Microscopy (TEM), and Zeta potential studies.
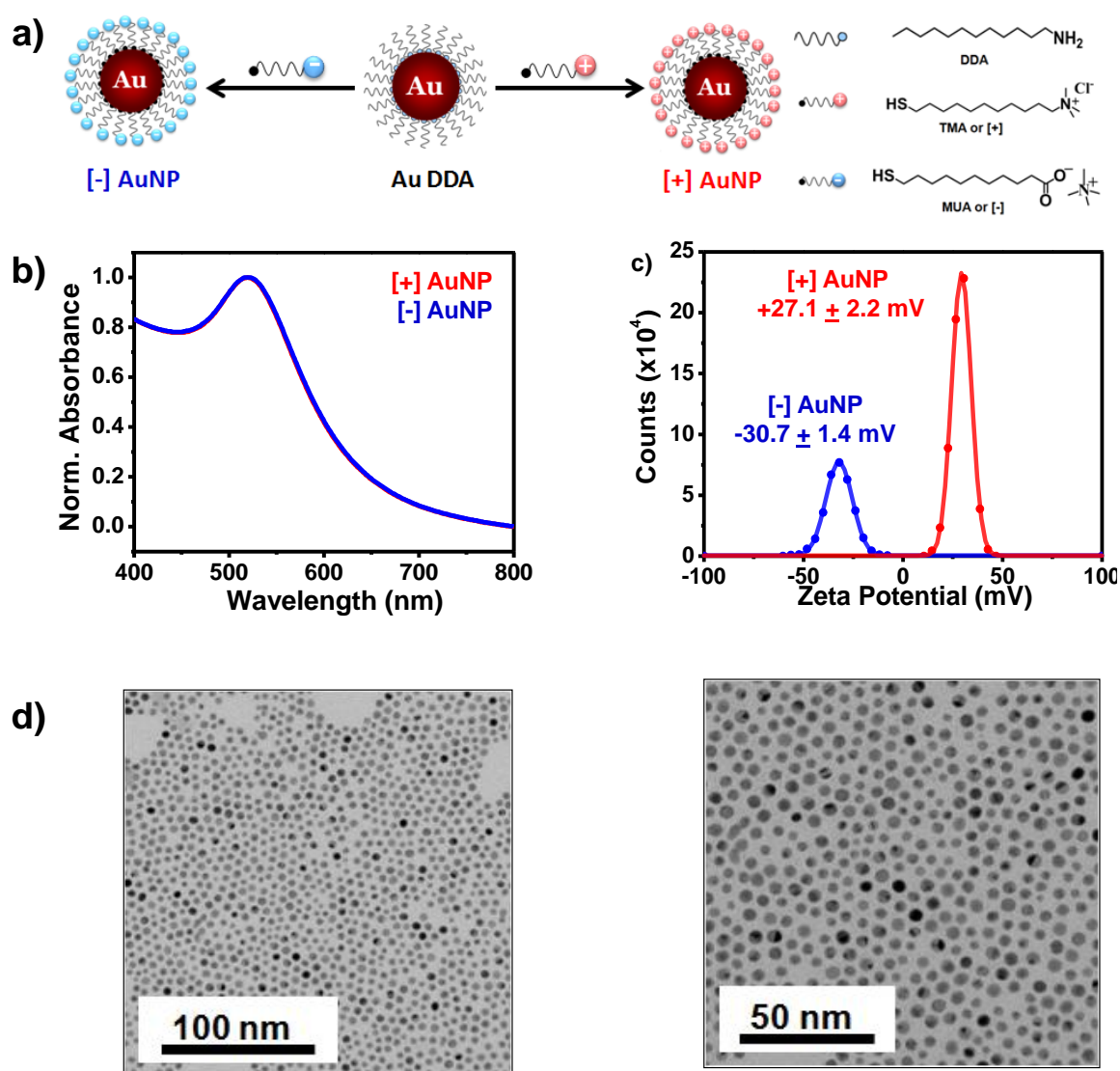

Figure 3.1 (a) Schematic showing the synthesis of [+] and [-] AuNPs via place exchange from Au-DDA to obtain positively and negatively charged nanoparticles

respectively. **(b)** Absorbance spectra of the [+] (red spectrum) and [-] (blue spectrum) AuNPs after place exchange. **(c)** Zeta potentials of the [+] and [-] AuNPs were estimated to be +27.1 ± 2.2 mV and -30.7 ± 1.4 mV, respectively. **(d)** Representative TEM image of [+] AuNPs with a mean diameter of 4.7 ± 0.5 nm (sample of 200 particles).

Figure 3.1 (b) shows negligible change in the absorption spectrum of [+] and [-] AuNPs after the place exchange reaction. Zeta potential studies carried on [+]and [-] AuNPs clearly show the presence of positive (+27.1 ± 2.2 mV values) and negative (-30.7 ± 1.4 mV values) surface charges on AuNPs, respectively (**Figure 3.1 (c)**). The average size of prepared AuNPs was estimated to be 4.7 ± 0.5 nm. These oppositely charged AuNPs were then titrated with each other to prepare inter-nanoparticle precipitates, as reported by Grzybowski and coworkers.[20]

3.2 The System: [+] – [-] Au nanoionic precipitates

We prepared [+] – [-]Au nanoionic precipitates ([+] – [-] AuNP ppt.) by titrating ~ 6nM of [+] AuNPs (**Figure 3.2 (b)**, red spectrum) with ~ 0.07 equivalent aliquots of [-] AuNPs.
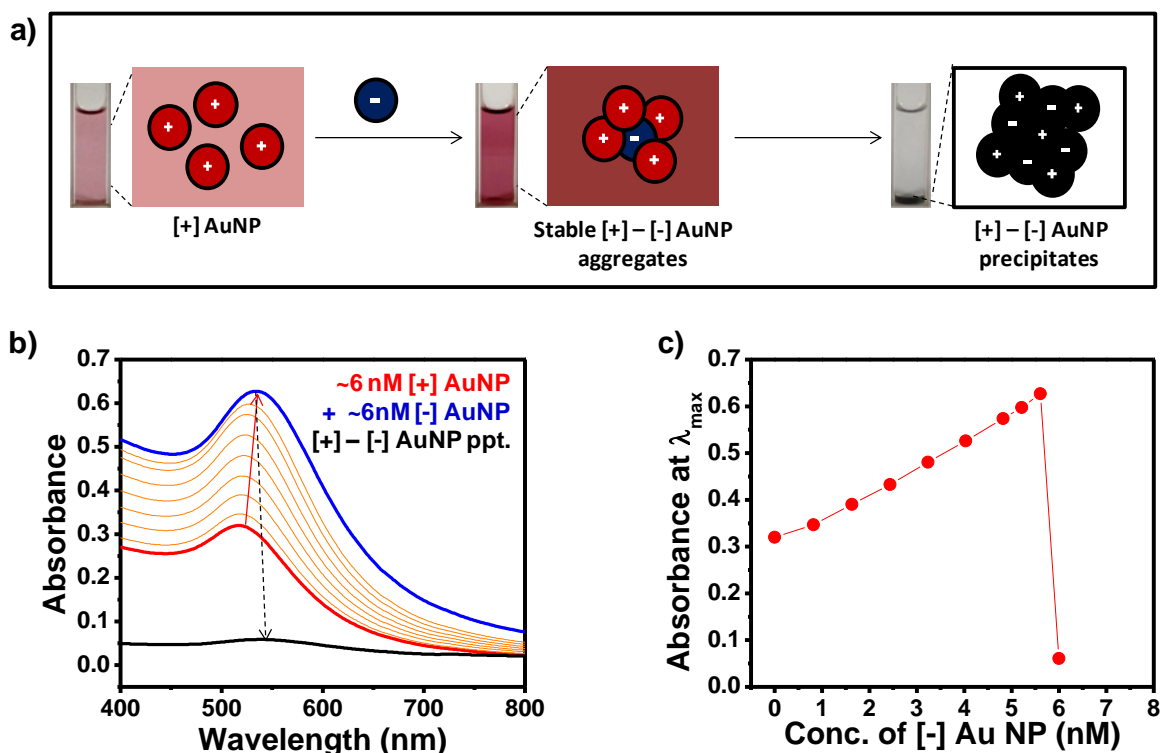
a)

[+] AuNP   Stable [+] – [-] AuNP aggregates   [+] – [-] AuNP precipitates

b)

~6 nM [+] AuNP
+ ~6nM [-] AuNP
[+] – [-] AuNP ppt.

Absorbance

Wavelength (nm)

c)

Absorbance at λ_{max}

Conc. of [-] Au NP (nM)

Figure 3.2 (a) Schematic showing the synthesis of [+] − [-] AuNP ppts. [+] AuNP was titrated with small aliquots of [-] AuNP. The nanoparticles form aggregates, and there was an increase in the plasmon intensity, which disappears on attaining electroneutrality. **(b)** The absorbance spectra taken during the titration. The starting point is ~ 6 nM of [+] AuNP (red spectrum). The increase in the plasmon intensity and gradual red shift in λ_{max} (shown by red arrow) occurs till the addition of ~ 6 nM [-] AuNP (blue spectrum), followed by a sharp precipitation (shown by dotted black arrow; black spectrum). **(c)** The intensity at λ_{max} showing the increase in plasmon intensity with increasing concentration of [-] AuNP and immediate precipitation at electroneutrality.

After each addition, there was a gradual red shift in the λ_{max} of the plasmon peak, accompanied by an increase in the intensity of the absorbance spectrum. This indicates aggregation, and subsequent plasmon coupling due to electrostatic attractions between oppositely charged AuNPs. Upon addition of ~ 6nM of [-] AuNPs, at the electroneutrality condition ($\Sigma Q_+ + \Sigma Q_- = 0$), there was a sudden precipitation of AuNPs from the solution accompanied by an abrupt loss of the plasmon band[20] (**Figure 3.2 (b)**, black spectrum). **Figure 3.2 (c)** shows the sharp fall in the absorbance at λ_{max} upon addition of ~ 6 nM [-] AuNPs).

3.3 Selectivity Studies in Medium with Lower Ionic Strength (Water)

Selectivity studies were first carried out in water (low ionic strength medium) by sequentially adding increasing amounts of Pb^{2+} ions and monitoring the response of [+] − [-] AuNP ppt. using UV-Vis. Spectroscopy (**Figure 3.3 (a)**). We observed a clear reappearance of wine red color upon the addition of ~ 1.5mM Pb^{2+} (limit of detection (LOD), **Figure 3.3 (b)**, blue spectrum corresponding to ΔAbs at λ_{max} ~0.05). Furthermore, we observed ~ 80% revival in the plasmon intensity upon addition of 10 mM Pb^{2+} (**Figure 3.3 (b)**, green spectrum). Selectivity studies were then carried out at 1.5 mM (**Figure 3.3 (c)**) and 10 mM M^{2+} concentrations (**Figure 3.3 (d)**), corresponding to minimum and maximum amount of Pb^{2+} that could be identified with the present system.
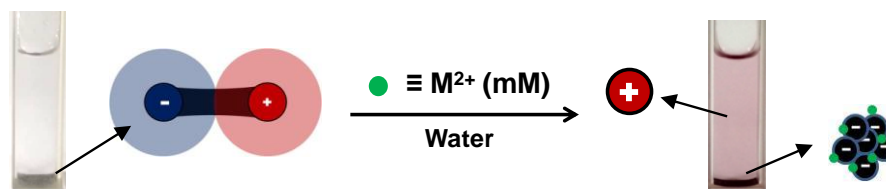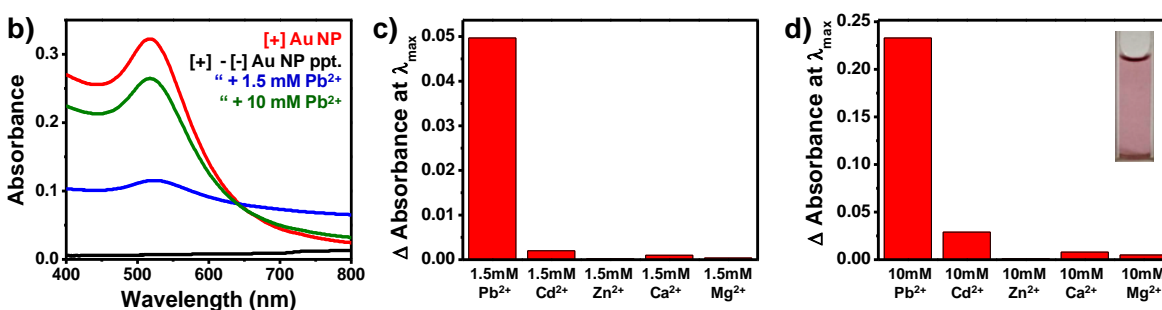
a)

Sensing Mechanism at Lower Ionic Strength

● ≡ M^{2+} (mM)

Water

M^{2+} : Pb^{2+} (✓), Cd^{2+} (✗), Zn^{2+} (✗), Ca^{2+} (✗), Mg^{2+} (✗)

Studies performed in Water (Ionic Strength ~ 0)

b) [+] Au NP / [+] - [-] Au NP ppt. / " + 1.5 mM Pb^{2+} / " + 10 mM Pb^{2+}

Absorbance vs Wavelength (nm)

c) Δ Absorbance at λ_{max} : 1.5mM Pb^{2+}, 1.5mM Cd^{2+}, 1.5mM Zn^{2+}, 1.5mM Ca^{2+}, 1.5mM Mg^{2+}

d) Δ Absorbance at λ_{max} : 10mM Pb^{2+}, 10mM Cd^{2+}, 10mM Zn^{2+}, 10mM Ca^{2+}, 10mM Mg^{2+}

Figure 3.3 (a) Scheme showing the sensing mechanism at lower ionic strength. The stronger electrostatic interactions are depicted by the high Debye screening length. Thus, ~ mM amounts of Pb^{2+} are required to break the interactions and release the [+] AuNP into the solution (turn-on response). **(b)** Absorbance spectra showing the minimum (blue spectrum) and maximum (green spectrum) amount of Pb^{2+} that could be identified with the present system. Effect of different M^{2+} ions at **(c)** 1.5 mM and **(d)** 10 mM, showcasing the selectivity of [+] − [-] Au nanoionic precipitates for Pb^{2+}.

It was observed that at both these concentrations, the system retained its exclusivity towards Pb^{2+} ions over other M^{2+} ions (**Figure 3.4 (b)**, and **(c)**). Most notably, the system could differentiate between similar amounts of Cd^{2+} and Pb^{2+} ions, without the need of analyte specific ligands.[15] This selectivity stems from the preferential breaking of interactions in [+] − [-] AuNP ppt. by Pb^{2+}.[15] The system, although selective towards Pb^{2+}, can identify ~ 1.5 mM of Pb^{2+}. We worked towards improving the sensitivity of the present identification protocol by reducing the electrostatic interactions in [+] − [-] AuNP ppt. We adopted two strategies to improve the sensitivity of our identification protocol.

3.4 Strategy 1 – Controlling the Electrostatic Interactions as a Function of Ionic Strength

Since the identification strategy relies on breaking of the electrostatic interactions in the nanoionic precipitate by different M^{2+} ions, we hypothesized that at higher ionic strengths the electrostatics will weaken, and lead to improvements in the sensitivity of our identification system.[21] To this effect, we prepared [+] – [-] AuNP ppt. in water, and the supernatant was replaced with 50 mM $NaNO_3$ to carry out the identification studies. It was observed that the nanoionic precipitates retained their stability in this salt solution. Upon adding sequentially higher amounts of Pb^{2+}, a noticeable reappearance of wine red color was seen at ~150 μM (LOD, ΔAbs at λ_{max} ~0.05, blue spectrum in **Figure 3.4 (b)**). It was encouraging to observe that the LOD value improved by a factor of ~10, when compared to the LOD value obtained in the medium of low ionic strength.
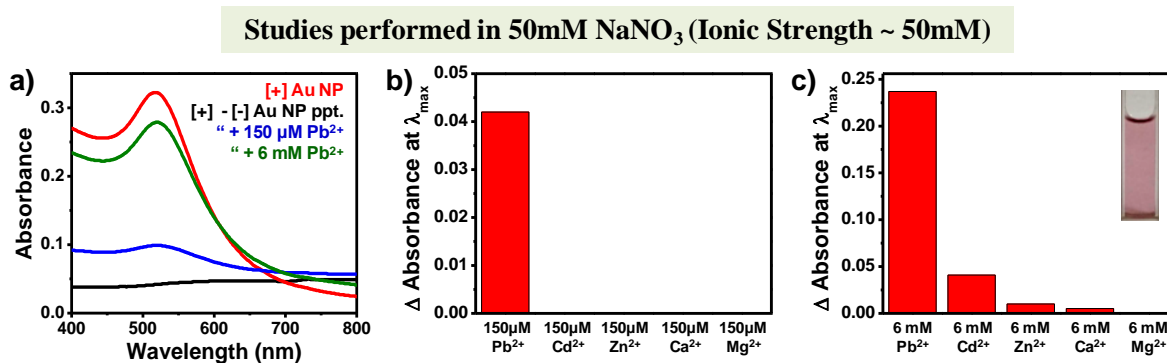

Figure 3.4 (a) Absorbance spectra showing the improved sensitivity of [+] − [-] nanoionic precipitates at higher ionic strength (50 mM $NaNO_3$). Selectivity studies at **(b)** 150 μM and **(c)** 6 mM showcasing the selectivity of the system for Pb^{2+}.

Further, ~80% of the plasmon intensity was revived upon the addition of 6 mM Pb^{2+}; ~1.6 times lower than what was observed in water (**Figure 3.4 (a)**, green spectrum). Interestingly, even at this high ionic strength, the nanoionic precipitates retained selectivity towards Pb^{2+} over Cd^{2+}, as 6 mM Cd^{2+} could only revive ~14% of the plasmon intensity **Figure 3.4 (c)**). Furthermore, detailed selectivity studies were carried out with different ions at 150 μM (**Figure 3.4 (b)**), and 6 mM (**Figure 3.4 (c)**) concentrations of M^{2+}, where minimum, and maximum amounts of Pb^{2+} could be

identified respectively. It was observed that at both these concentrations, the system demonstrated selectivity towards Pb^{2+}.

To invariably establish the role of ionic strength in improving the sensitivity of the identification protocol, we systematically varied the concentration of $NaNO_3$ (electrolyte) in the solution and titrations were performed with Pb^{2+} (**Table 3.1**). It was observed that with an increase in ionic strength, lower amounts of Pb^{2+} could be visually detected; ~50 fold improvement, from 1.5 mM to 30 µM in LOD was observed while going from 0 to 300 mM $NaNO_3$ as shown in **Table 1**. These LOD values are comparable to the best reported values by a non-selective carboxylate functionalized AuNP system.[9–13] Furthermore, lower amounts of Pb^{2+} were required to give the maximum revival of plasmon intensity (~5 fold improvement), as shown in **Table 3.1.** From above results, it can be inferred that sensitivity of [+] – [-] AuNP ppt. can indeed be improved by increasing the ionic strength of the surrounding medium!

[NaNO$_3$]	[Pb^{2+}]$_{LOD}$	[Pb^{2+}]$_{Max.}$	Plasmon Revival
0	1.5 mM	10 mM	78 %
1 mM	1.25 mM	10 mM	70 %
5 mM	500 µM	7 mM	71 %
10 mM	300 µM	4 mM	71 %
50 mM	150 µM	6 mM	80 %
200 mM	50 µM	1 mM	68 %
300 mM	30 µM	2 mM	74 %

Table 3.1 Effect of variation in ionic strength of the medium on the LOD (second column) as well as maximum (third column) amount of Pb^{2+} that could be detected.

In order to check if the system retained its selectivity towards Pb^{2+}, we performed detailed selectivity studies with M^{2+} ions at 30 µM (**Figure 3.5 (b)**) and 2 mM (**Figure 3.5 (c)**) concentrations of M^{2+} where minimum, and maximum amounts of Pb^{2+} could be identified respectively. It was observed that the system remained exclusively selective towards Pb^{2+} over other M^{2+} ions at both the concentrations (LOD, maximum revival). Interestingly, even a mixture of other M^{2+} ions (Cd^{2+}, Ni^{2+}, Ba^{2+}, Zn^{2+} and Ca^{2+})

was unable to break the interparticle interactions in [+] – [-] AuNP ppts. (**Figure 3.5 (b)**).
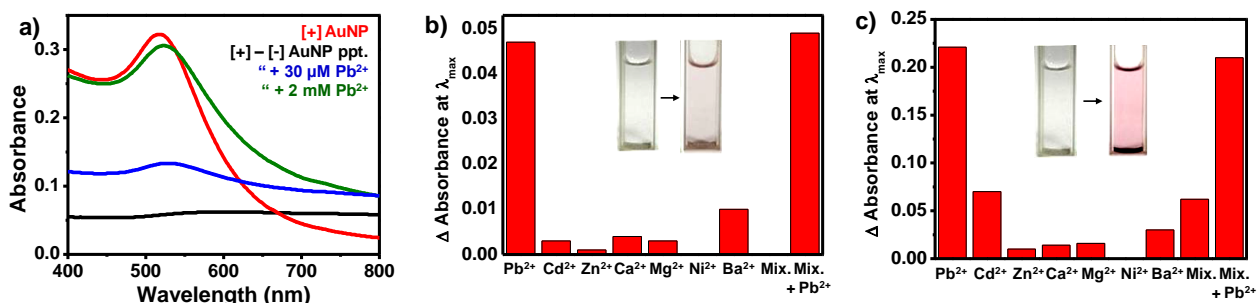

Figure 3.5 (a) Absorbance spectra showing the improved sensitivity levels for Pb^{2+} in 300 mM $NaNO_3$. Selectivity studies at **(b)** 30 µM and **(c)** 2 mM M^{2+} concentrations. The insets in **(c)** and **(d)** show the development of colour on addition of LOD and maximum concentrations of Pb^{2+}, respectively. In the latter case, the black precipitates of [-] AuNP-Pb^{2+} are still visible.

However, a revival of plasmon band was observed only when 30 µM of Pb^{2+} was included in the mixture (**Figure 3.5 (b),** Mix. + Pb^{2+} gave ΔAbs. ~0.05 at λ_{max}). At the higher concentration (2 mM) where Pb^{2+} gives the maximum revival of plasmon intensity, it was seen that Cd^{2+} gives the visible colour change, while all the other ions remain undetected. Interestingly, mixture of other M^{2+} ions (Cd^{2+}, Ni^{2+}, Ba^{2+}, Zn^{2+} and Ca^{2+}) also showed minimal visible color change (because of Cd^{2+}), but ~ 70% revival of plasmon intensity occurred only when Pb^{2+} was included in the mixture. The entire process of preferential breaking of interparticle interactions in [+] – [-] AuNP ppts was monitored by microscopic studies as well. **Figure 3.6 (a)** and **(b)** shows TEM and SEM images of individual [+] AuNPs (left) and [+] – [-] AuNP ppt. upon addition of equimolar amount of [-] AuNPs (center). Upon addition of µM amount of Pb^{2+}, [+] AuNPs leaked out into the solution (individual AuNPs shown in right). Additionally, we observed the presence of large ~µm sized [-] AuNP – Pb^{2+} precipitates.
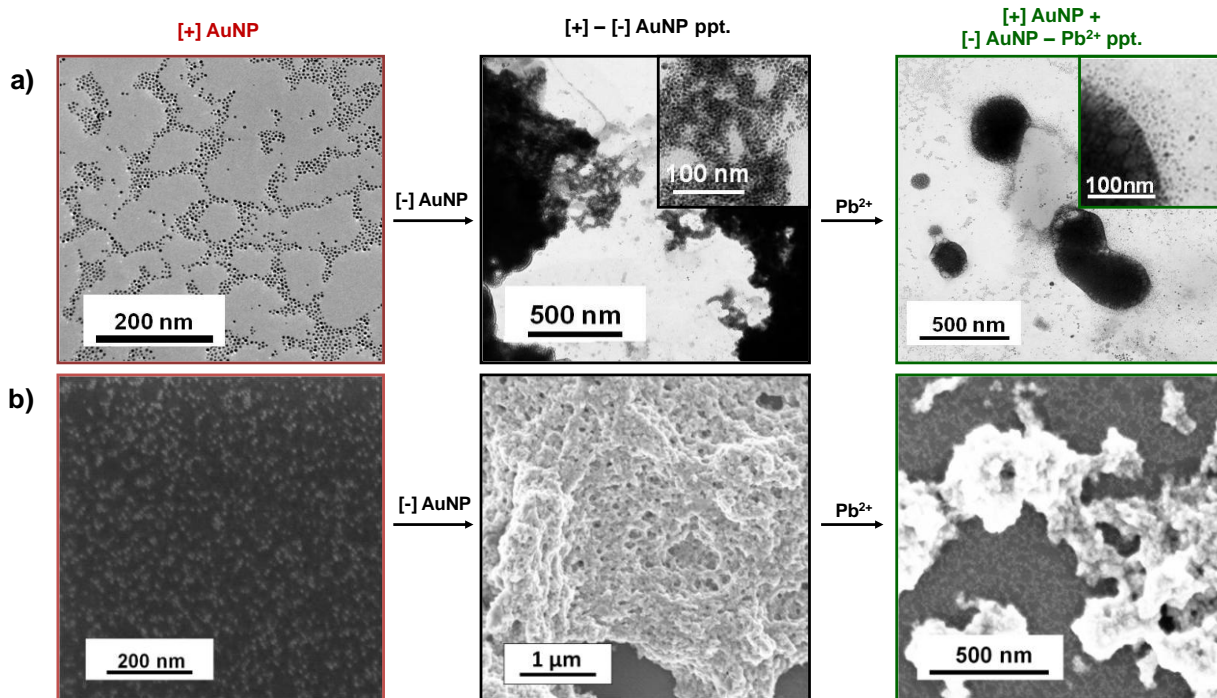
Figure 3.6 (a) TEM images and **(b)** SEM images showing [+] AuNP, which form [+] − [-] AuNP ppt. on addition of [-] AuNP. The precipitates break to release the [+] AuNPs in the presence of Pb^{2+} (the amount of Pb^{2+} added was such that it gave the maximum revival)

According to our hypothesis, Pb^{2+} was able to displace [+] AuNPs from the [+] − [-] AuNP ppt due of its superior interactions with [-] AuNPs. At higher ionic strength, displacement of [+] AuNPs by Pb^{2+} happens at μM concentrations, as shown in **Figure 3.7 (a)**. This was confirmed by comparing the zeta potential of the redispersed solution, upon addition of Pb^{2+} (**Figure 3.7 (b)**). It can be seen from **Figure 3.7 (b)** that the zeta potential value for the redispersed solution was positive (+26.2 ± 0.6 mV), and moreover similar to that of the initial [+] AuNPs.

Sensing Mechanism at Higher Ionic Strength
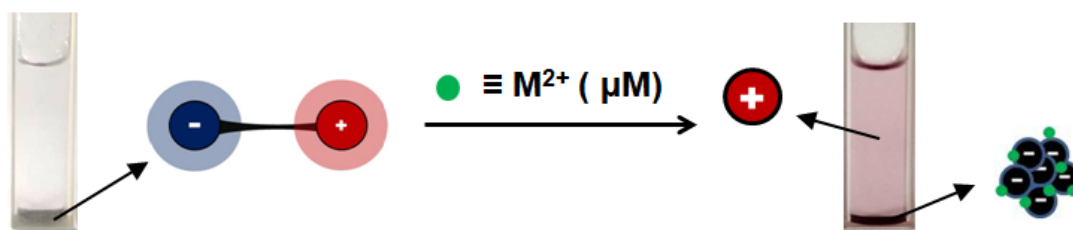
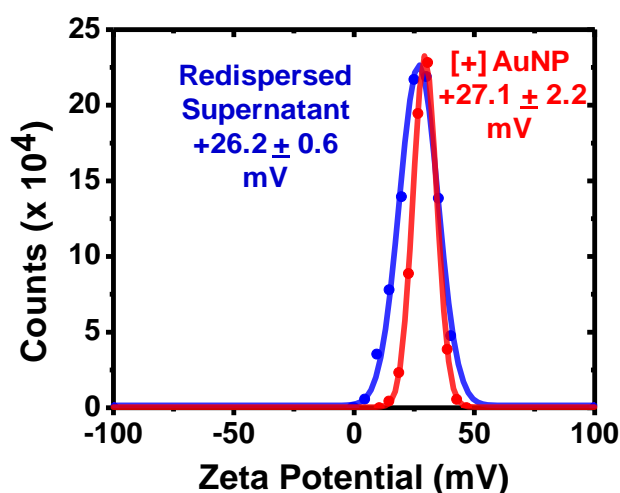M^{2+} : Pb^{2+} (✓), Cd^{2+} (✗), Zn^{2+} (✗), Ca^{2+} (✗), Mg^{2+} (✗)

Figure 3.7 (a) Schematic showing the proposed mechanism at higher ionic strength. The Debye screening length is shown to be lower as compared to in water, thus reducing the electrostatic interactions. Consequently, lesser amounts of Pb^{2+} (~ μM) are required to break the interactions (compared to water) and release [+] AuNP into the solution. **(b)** Zeta potential of the redispersed supernatant (blue graph with mean zeta potential at +26.2 ± 0.6 mV) in 10 mM $NaNO_3$ at maximum plasmon revival. The zeta potential of initial [+] AuNP is shown for comparison (red graph with mean zeta potential at +27.1 ± 2.2 mV). The similarity in the mean zeta potential values suggest that [+] AuNP was released into the solution in the presence of Pb^{2+}.

To ensure the generality of our identification protocol, we performed selectivity studies in a different electrolyte, namely Potassium Nitrate (KNO_3), at the same ionic strength (300 mM) (**Figure 3.8**). The sensitivity of the [+] – [-] AuNP ppt. for Pb^{2+} was similar to what was obtained in 300 mM $NaNO_3$. The LOD was ~40 μM (**Figure 3.8,**

blue spectrum) and the maximum amount of Pb^{2+} detected was ~ 2 mM, but with a revival in plasmon intensity of ~ 65 %. The selectivity studies were carried out at 40 µM and 2 mM, corresponding to minimum and maximum amount of Pb^{2+} that could be identified. At ~ 40 µM, the system showed a visible colour change only in the presence of Pb^{2+} (**Figure 3.8 (a)**, blue spectrum). Further, addition of 2 mM Pb^{2+} resulted in ~65 % revival of plasmon color to the solution (**Figure 3.8 (a)**, green spectrum). Detailed selectivity studies with M^{2+} ions were then performed at 40 µM (**Figure 3.8 (b)**) and 2 mM (**Figure 3.8 (c)**), where minimum and maximum amounts of Pb^{2+} could be identified respectively. It was observed that the system remained exclusively selective towards Pb^{2+} over other M^{2+} ions at 40 µM (LOD). Interestingly, even a mixture of other M^{2+} ions (Cd^{2+}, Ni^{2+}, Ba^{2+}, Zn^{2+} and Ca^{2+}) was unable to break the interparticle unless 40 µM Pb2+ was added to the mixture. At the higher concentration (2 mM) where Pb^{2+} gives the maximum revival of plasmon intensity, it was seen that Cd^{2+} gives the minimum visible colour change, while all the other ions remain undetected. Interestingly, mixture of other M^{2+} ions (Cd^{2+}, Ni^{2+}, Ba^{2+}, Zn^{2+} and Ca^{2+}) also showed minimal visible color change (because of Cd^{2+}), but ~ 65 % revival of plasmon intensity occurred only when Pb^{2+} was included in the mixture. These studies confirm that our hypothesis of improved sensitivity at higher ionic strengths is independent of the identity of the electrolyte.

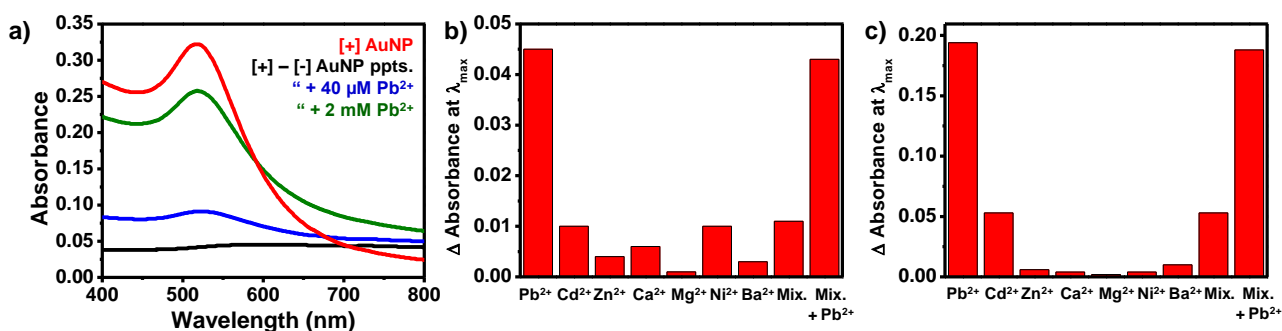**Figure 3.8 (a)** Absorbance spectra showing the LOD and maximum levels at which Pb^{2+} is detected in 300 mM KNO$_3$. Selectivity studies at **(b)** 40 µM and **(c)** 2 mM ion concentration for individual ions as well as for mixtures of ions.

3.5 Strategy 2 - Controlling the Electrostatic Interactions as a Function of Surface Charge

As described previously, the sensitivity of the present identification protocol can be conveniently modified by tuning the strengths of electrostatic interactions holding the [+] – [-] AuNP ppt. In this direction, we have already discussed in the previous section the effectiveness of the ionic strength of the surrounding solution as a convenient means to tune the electrostatic attractions, and ultimately the sensitivity of [+] – [-] AuNP ppt. Next, we discuss an alternative way to tune the electrostatic interactions – by preparing nanoionic precipitates between a homogeneously charged [+] AuNP and heterogeneously charged [+/-] AuNP. Accordingly, we synthesized [+/-]$_9$ AuNPs by place exchanging DDA capped AuNPs with a 1:9 mixture of [+], and [-] ligands. Nanoionic precipitates formed from such AuNPs, because of electrostatic repulsions between quaternary ammonium ions, will have lower electrostatic attractions in [+] – [+/-]$_9$ AuNP ppt, when compared to [+] – [-] AuNP ppt. We studied the response of such weakly bound nanoionic precipitates towards M^{2+} ions in solutions of high ionic strengths.

3.6 Synthesis of [+/-]$_9$ AuNP

The as synthesized [+/-]$_9$ AuNPs were characterized by UV-Vis. absorbance, zeta potential and TEM studies. **Figure 3.9 (b)** shows presence of typical surface plasmon absorption peak at ~520 nm corresponding to un-aggregated AuNPs. **Figure 3.9 (c)** shows that the zeta potential value of [+/-]$_9$ falls in between that of [+] and [-] AuNPs. Further, a net negative value of -17.2 ± 0.8 mV demonstrates the presence of higher amounts of [-] on the surface of [+/-]$_9$ AuNPs over [+]. The average size of the nanoparticles was estimated to be 4.7 ± 0.5 nm (**Figure 3.9 (d)**). The on-nanoparticle ratio was estimated to be [+/-]$_7$ based on our previous studies.[18]
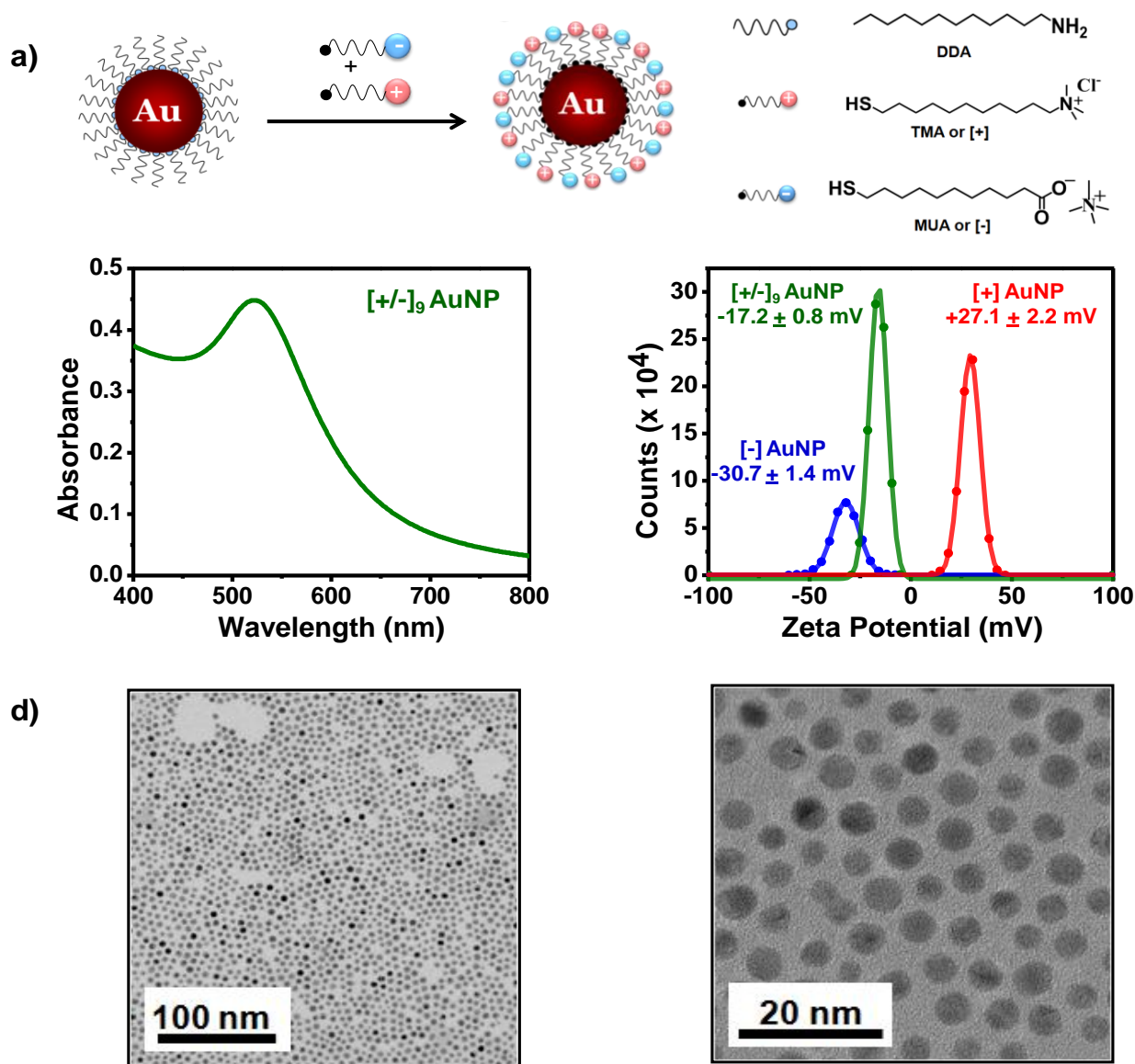
Figure 3.9 (a) Schematic showing the synthesis of [+/-]$_9$ AuNP from Au-DDA via place exchange method, in which the ligands are added in the ratio [+] : [-] = 1 : 9. **(b)** Absorbance spectrum of [+/-]$_9$ AuNP with λ_{max} of the plasmon peak at ~ 520 nm. **(c)** Zeta potential of the [+/-]$_9$ AuNP showing a charge distribution with mean value -17.2 ± 0.8 mV (green graph). The zeta potentials of [+] AuNP (red graph) and [-] AuNP (blue graph) are given for comparison **(d)** Representative TEM image of [+/-]$_9$ AuNPs. The average size of the nanoparticles was estimated to be 4.7 ± 0.5 nm.

3.7 The System: [+] – [+/-]$_9$ Nanoionic Precipitates

Nanoionic precipitates between homogeneously charged [+] and heterogeneously charged [+/-]$_9$ AuNPs were prepared in a way similar to [+] – [-] AuNP ppt. Briefly, ~ 6

nM of [+/-]$_9$ AuNPs were titrated with ~ 0.07 equivalents aliquots of [+] AuNP. Analogous to [+] − [-] AuNP ppt., with each addition, there was a gradual bathochromic shift in the plasmon peak. This process continued till the concentration of [+] AuNP in the solution became ~ 4 nM, at which the nanoparticles precipitated sharply from the solution forming [+] − [+/-]$_9$ AuNp ppt. (**Figure 3.10 (a), (b)**). **Figure 3.10 (b)** shows the variation in absorbance at λ_{max} versus concentration of [+] AuNPs added.
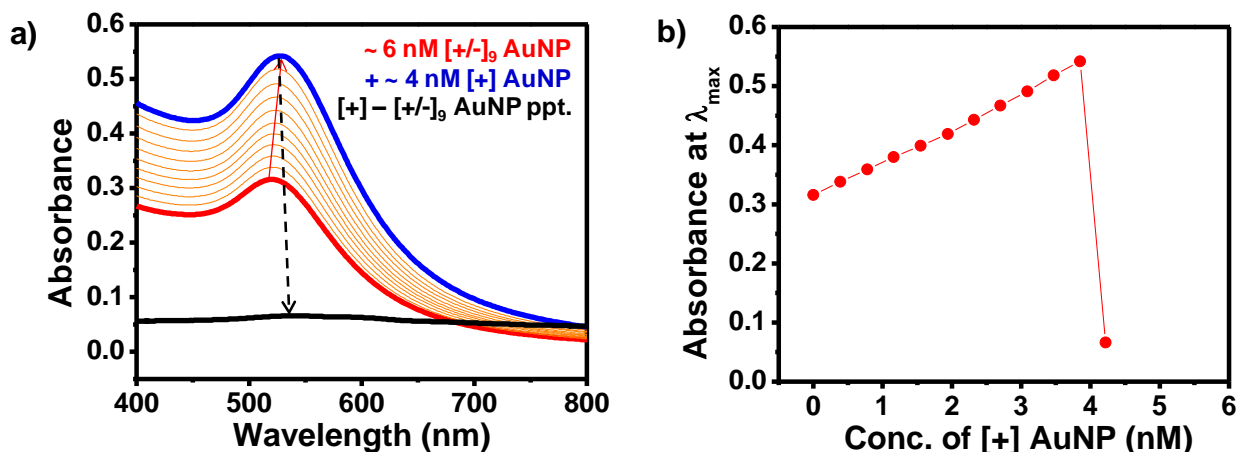

Figure 3.10 (a) Absorbance spectra showing the changes taking place during the titration of [+/-]$_9$ AuNP (red spectrum) with [+] AuNP. The absorbance intensity increases till ~ 4 nM, at which electroneutrality is reached following which it undergoes a sharp decrease. **(b)** Graphical representation showing the changes in absorbance intensity at λ_{max} as a function of increasing [+] AuNP concentration. The sharp reduction in intensity occurs when ~ 4 nM [+] AuNPs was added to the solution.

3.8 Optimization of Ionic Strength

We studied the stability of [+] − [+/-]$_9$ AuNP ppt. in varying electrolyte concentrations (See **Figure 3.11**), to test the stability of [+] − [+/-]$_9$ AuNP ppt. at high ionic strengths. The precipitates were synthesized in water, and the supernatant was replaced with different concentrations of NaNO$_3$, ranging from 300 mM to 20 mM. **Figure 3.11** clearly demonstrate that out of all tested concentrations of NaNO$_3$, the [+] − [+/-]$_9$ AuNP ppts. were stable in only 20 mM of NaNO$_3$ (**Figure 3.11**, green spectrum).
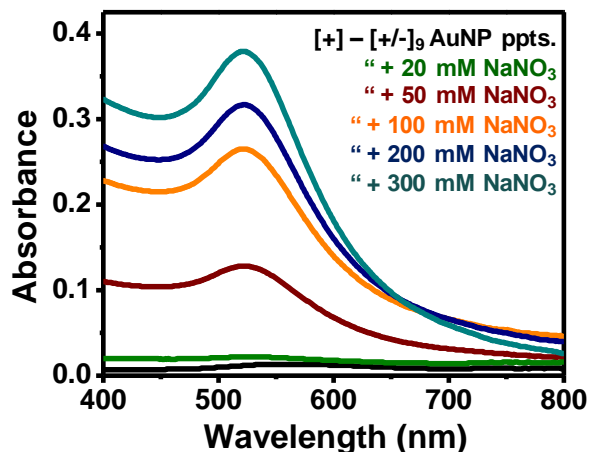
Figure 3.11 Absorbance spectra showing the stability of $[+] - [+/-]_9$ AuNP ppt. in different concentrations of $NaNO_3$. As seen from the graph, the $[+] - [+/-]_9$ AuNP ppts were not stable at concentrations greater than 20 mM of $NaNO_3$.

Following this, we conducted M^{2+} binding studies in 20 mM to determine the sensitivity of $[+] - [+/-]_9$ AuNP ppt. for Pb^{2+} ions. Upon adding sequentially higher amounts of Pb^{2+}, a noticeable reappearance of wine red color was seen at ~0.5 μM (LOD, ΔAbs at λ_{max} ~0.05, blue spectrum in **Figure 3.12 (a)**). This LOD value, which is ~ 60 fold improvement compared to the best value we have obtained so far (~ 30 μM in 300 mM $NaNO_3$ for $[+] - [-]$ system). Unfortunately, the system did not display selectivity for Pb^{2+}, since even the mixture of ions (Zn^{2+}, Ca^{2+}, Mg^{2+}, Ni^{2+} and Ba^{2+}) without Pb^{2+} and Cd^{2+} also gave a similar visible colour change (**Figure 3.12 (a)**, orange spectrum). These studies rule out the use of 20 mM $NaNO_3$ as the working medium.

On reducing the ionic strength of the medium to 10 mM, the $[+] - [+/-]_9$ AuNP ppt. displayed a sensitivity of ~ 1 μM, which is a ~ 30 fold improvement compared to the sensitivity of the $[+] - [-]$ AuNP ppt. in 300 mM $NaNO_3$. Interestingly, this system did not show any response when exposed to a 1 μM mixture of ions (Zn^{2+}, Ca^{2+}, Mg^{2+}, Ni^{2+} and Ba^{2+}). However, it failed to differentiate between Pb^{2+} and Cd^{2+} making this medium also unfit for our use (**Figure 3.12 (b)**).
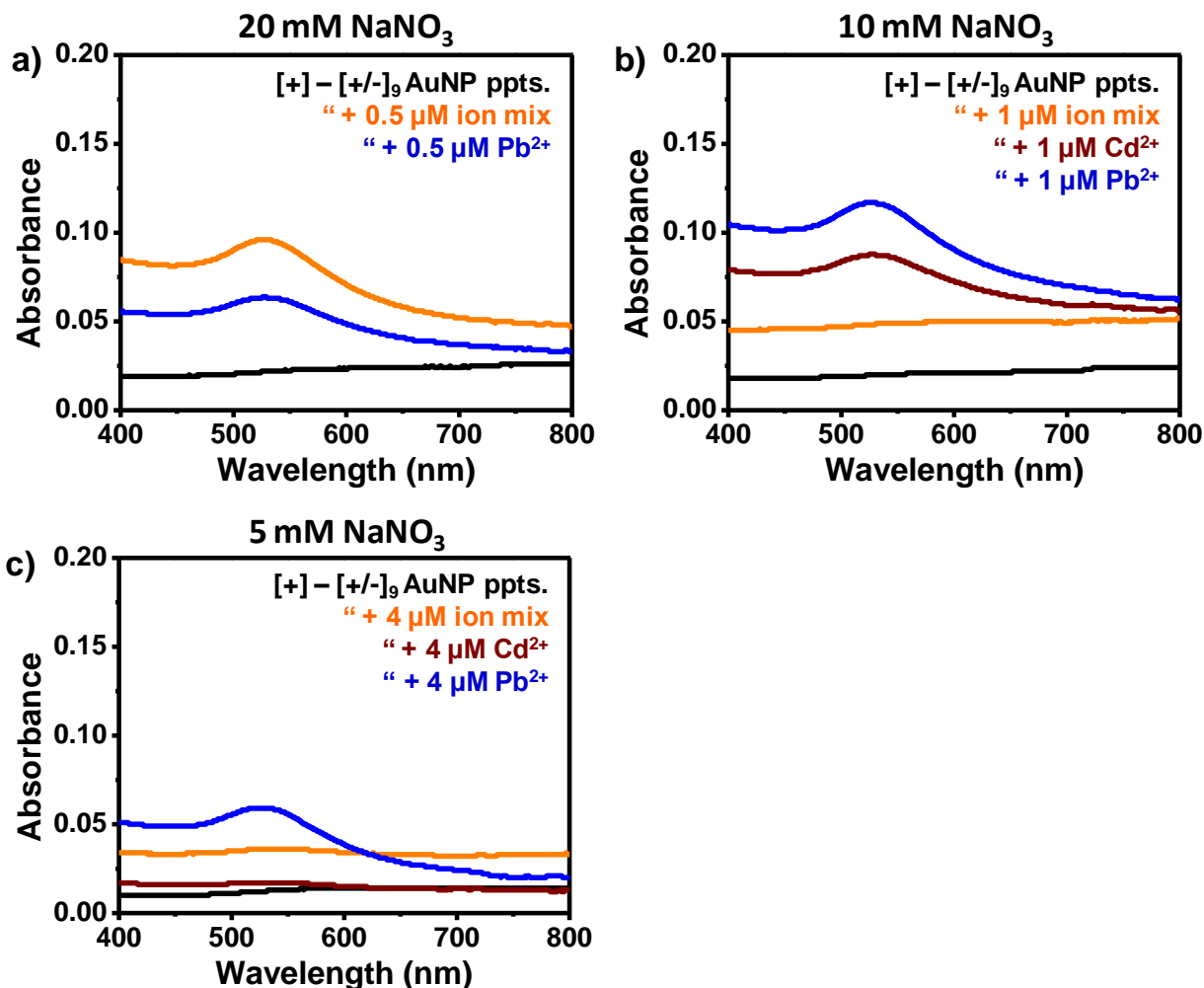
Figure 3.12 (a) M^{2+} binding studies in 20 mM $NaNO_3$ showing improved sensitivity for Pb^{2+} (blue spectrum); but no selectivity since even the mixture of ions without Pb^{2+} and Cd^{2+} were able to give a visible colour change. **(b)** Studies in 10 mM $NaNO_3$ where the LOD for Pb^{2+} was ~ 1 μM. The ion mixture without Pb^{2+} and Cd^{2+} was undetected (orange spectrum). A visible colour change occurred in the presence of ~ 1 μM Cd^{2+} as well (brown spectrum), thus compromising the selectivity for Pb^{2+}. **(c)** Studies in 5 mM $NaNO_3$ where the system displays selectivity for Pb^{2+} (blue spectrum with Δ Abs. ~ 0.05), while both the mixture of ions (orange spectrum) and Cd^{2+} (brown spectrum) were undetected.

On further reducing the ionic strength to 5 mM $NaNO_3$, we found the sensitivity of the system towards Pb^{2+} to be ~4 μM (**Figure 3.13 (a)**)**,** which is ~ 8 times better than the best value compared to [+] − [-] AuNP ppt. in 300 mM $NaNO_3$. Moreover, this value is better or on par with other nanoparticle systems with non-analyte specific ligands.[9–13] The maximum revival occurred at ~ 4 mM Pb^{2+} (**Figure 3.13 (a)**, green spectrum), but

there was no selectivity at this concentration (**Figure 3.13 (c)**). The intensity of the resultant spectrum was found to be higher than the individual nanoparticle spectra (**Figure 3.13 (a)**), red dotted spectrum corresponding to [+/-]$_9$ AuNP and purple dotted spectrum corresponding to [+] AuNP) indicating the complete redispersal of [+] – [+/-]$_9$ precipitates unlike the partial redispersal of [+] – [-] system. The [+] AuNPs were released into the solution along with [+/-]$_9$ – Pb^{2+} agregates.[19] This is also evident from the red shift at λ_{max} of the final redispersed sample compared to the individual nanoparticle samples.
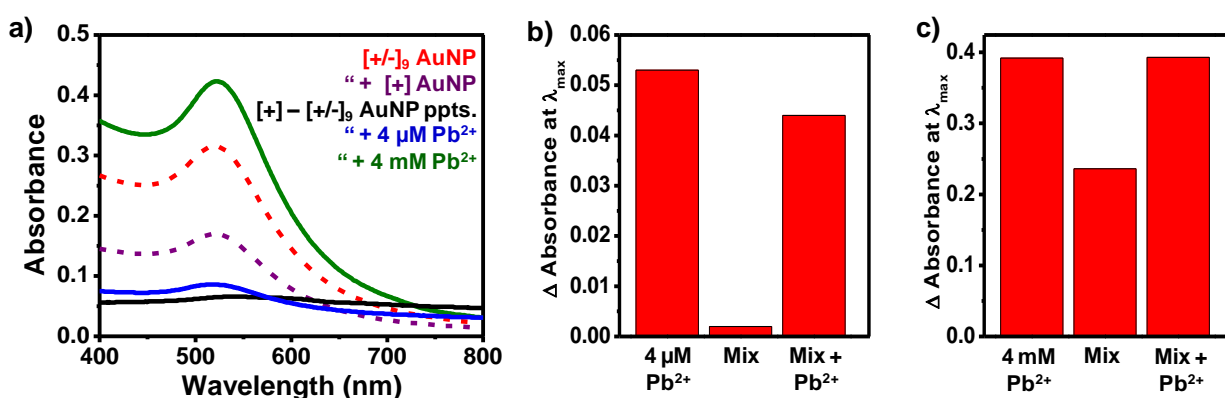

Figure 3.13 (a) Absorbance spectra showing the LOD and maximum levels at which Pb^{2+} was detected, which were 4 µM (blue spectrum) and 4 mM (green spectrum) respectively in 5mM NaNO$_3$. **(b)** The system shows selectivity for Pb^{2+} at the LOD concentration of 4 µM. Colour change is only observed in the presence of Pb^{2+}, either independently or when present in the mixture of ions. **(c)** The selectivity study at the maximum limit (4 mM) reveals a loss in the selectivity since the ion mixture without Pb^{2+} shows a visible colour change.

According to our hypothesis, Pb^{2+} breaks the electrostatic interactions holding the [+] – [+/-]$_9$ AuNP ppt. leading to redispersal of both homogeneously and heterogeneously charged AuNPs to the solution. We observed that the zeta potential of the redispersed solution, upon addition of Pb^{2+}, to be 29.7 ±0.3 mV **(Figure 3.14)**. This net positive zeta potential value is due to the presence of [+] AuNP and [+/-]$_9$ AuNP–Pb^{2+} aggregates in the solution.
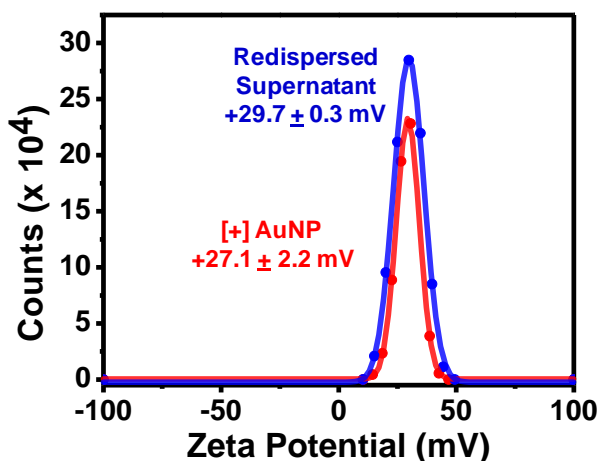
Figure 3.14 Zeta potential of the redispersed supernatant (blue graph with mean zeta potential at +29.7 ± 0.3 mV) in 5 mM $NaNO_3$ at maximum plasmon revival. The zeta potential of initial [+] AuNP is shown for comparison (red graph with mean zeta potential at +27.1 ± 2.2 mV).

In conclusion, we have summarized our results in the following table (**Table 3.2**), comparing the sensitivity of our system with previously reported systems.

The first five reports of previously reported carboxylate functionalized sensors (**Table 3.2**) showed ~µM sensitivity towards Pb^{2+}. But these systems either did not show any selectivity or did so only in the presence of a specific molecule. The next two reports ([+] - [-] AuNP ppt and [+] - [+/-]$_9$ AuNP ppt, **Table 3.2**) are the results of previous work carried out in the group, where the aspect of selectivity was addressed by using the preferential breaking of electrostatic interactions as the detection strategy. But, the sensitivity of this system towards Pb^{2+} was ~mM, which needed improvement. This improvement in the sensitivity was achieved with the present work (**Table 3.2**) where the sensitivities of both [+] - [-] AuNP ppt. and [+] - [+/-]$_9$ AuNP ppt. were improved by tuning the electrostatic interactions. Through our present study, the sensitivity of the [+] - [-] AuNP ppt. was improved by an order of magnitude compared to the previous report by varying the ionic strength (I): previously reported LOD of 1 mM was improved to ~30 µM in medium of I ~300 mM. The best value that we obtained was ~4 uM, by simultaneously varying the surface chemistry and the ionic strength ([+] - [+/-]$_9$ AuNP

ppt. in medium of I ~20 mM). Both these values which we obtained from the present work are comparable or better than the previously reported ones, along with the added advantage of selectivity without the aid of analyte specific ligand or specific molecules.

M^{2+}	Nanoparticle System	LOD	Selectivity	Reference
Pb^{2+}	MUA – AuNPs	400 μM	No	*Nano Lett.* **2001,** *1,* 165–167
Pb^{2+}	Gallic acid – AuNPs	5 – 150 μM	No	*J. Phys. Chem. C* **2007,** *111,* 12839–1284
Pb^{2+}	MUA – AuNPs	10 μM	No	*Sensors* **2012,** *12,* 9467–9475
Pb^{2+}	MUA – AuNPs (amino acids)	2 – 50 μM	Yes (additional specific molecule needed)	*ACS Appl. Mater. Interfaces* **2014,** *6,* 18395–18400
Pb^{2+}	MUA – AuNPs	> 50 μM	Yes (additional specific molecule needed)	*Anal. Methods.* **2016,** *8,* 7232–7236
Pb^{2+}	[+] – [+/-]$_9$ AuNP ppt.	~ 20 μM	Yes	ChemRxiv. **2018,** doi.org/10.26434/chemrxiv.7195817.v1
Pb^{2+}	[+] – [-] AuNP ppt.	~ 1 mM	Yes	ChemRxiv. **2018,** doi.org/10.26434/chemrxiv.7195817.v1
Pb^{2+}	**[+] – [-] AuNP ppt. (at I ~ 300 mM)**	**~ 30 μM**	**Yes**	**Present work**
Pb^{2+}	**[+] – [+/-]$_9$ AuNP ppt.(at I ~ 5 mM)**	**~ 4 μM**	**Yes**	**Present work**

Table 3.2 Comparison of the sensitivity of non-analyte specific nanoparticle systems towards Pb^{2+}

Chapter 4: Conclusion

In the work presented in this thesis, we have demonstrated the improvement in the sensitivity of an inherently non-selective nanoparticle system by careful manipulation of interparticle forces rather than the use of an analyte specific ligand. The force under consideration is the electrostatic interaction between the oppositely charged nanoparticles which form the nanoionic precipitate ([+] − [-] AuNP ppt.): the detection system. Since the detection strategy of this system was the preferential breaking of electrostatic interactions by M^{2+}, we hypothesized that by weakening these interactions, lower amounts of M^{2+} would be required, and hence leading to an improvement in the sensitivity. The first step towards this goal was to study the sensitivity as a function of ionic strength. And indeed, we did observe an improvement in the sensitivity of the [+] − [-] AuNP ppt. with increasing ionic strength, along with its selectivity intact. The LOD obtained for Pb^{2+} detection was ~ 30 μM at an ionic strength of 300 mM, which is an improvement by an order of magnitude. The second approach we took was to study the effect of surface charge on the sensitivity. For this, we used nanoionic precipitate containing a mixture of homogeneously and heterogeneously charged AuNPs ([+] − [+/-]$_9$ AuNP ppt.). By varying the surface charge in conjunction with the ionic strength, we could further lower the detection limit to ~ 4μM, which is comparable to/ better than most non-selective detection systems. Thus, in conclusion, we have improved the sensitivity of the nanoparticle system solely by tuning the interparticle forces, without the use of any analyte specific ligand.

References

(1)   Roduner, E. Size Matters : Why Nanomaterials Are Different. *Chem. Soc. Rev.***2006**, 35, 583–592.

(2)   Semiconductor Clusters, Nanocrystals, and Quantum Dots. Alivisatos A.P. *Science*, *271*, 934-937

(3)   Eustis, S.; El-sayed, M. A.; Kasha, M. Why Gold Nanoparticles Are More Precious than Pretty Gold : Noble Metal Surface Plasmon Resonance and Its Enhancement of the Radiative and Nonradiative Properties of Nanocrystals of Different Shapes. *Chem. Soc. Rev.* **2006**, 35, 209–217.

(4)   Amendola, V.; Pilot, R.; Frasconi, M. Surface Plasmon Resonance in Gold Nanoparticles : A Review. *J. Phys.: Condens. Matter* **2017**, *29*, 203002

(5)   https://nanocomposix.com/pages/gold-colloid.

(6)   Grassian, V. H. When Size Really Matters : Size-Dependent Properties and Surface Chemistry of Metal and Metal Oxide Nanoparticles in Gas and Liquid Phase Environments †. *J. Phys. Chem. C.* **2008**, 112, 18303–18313.

(7)   Ray, P. C. Size and Shape Dependent Second Order Nonlinear Optical Properties of Nanomaterials and Their Application in Biological and Chemical Sensing. *Chem. Rev.* **2010**, 110, 5332–5365.

(8)   Grzybowski, B. A.; Huck, W. T. S. The Nanotechnology of Life-Inspired Systems. *Nat. Nanotech.* **2016**, *11*, 585–592.

(9)   Kim, Y.; Johnson, R. C.; Hupp, J. T. Gold Nanoparticle-Based Sensing of " Spectroscopically Silent " Heavy Metal Ions. *Nano. Lett.* **2001**, 1, 165-167.

(10)   Yoosaf, K.; Ipe, B. I.; Suresh, C. H.; Thomas, K. G. In Situ Synthesis of Metal Nanoparticles and Selective Naked-Eye Detection of Lead Ions from Aqueous Media. *J. Phys. Chem. C.* **2007**, *111,*12839–12847.

(11)   Fan, C.; He S.; Liu, G.; Wang, L.; Song, S. A Portable and Power-Free M Icrofluidic Device for Rapid and Sensitive Lead (Pb 2+) Detection. *Sensors* **2012**, *12*, 9467–9475.

(12)   Sener, G.; Uzun, L.; Denizli, A. Colorimetric Sensor Array Based on Gold Nanoparticles and Amino Acids for Identification of Toxic Metal Ions in Water.

ACS. Appl. Mater. Interfaces **2014**, *6*, 18395-18400.

(13)   Zhu, R.; Song, J.; Ma, Q.; Zhou, Y.; Yang, J.; Shuang, S.; Dong, C. Analytical Methods Ions Based on 11-Mercaptoundecanoic Acid. *Anal. Methods* **2016**, *8*, 7232–7236.

(14)   Rao, A.; Roy, S.; Unnikrishnan, M.; Bhosale, S. S.; Devatha, G.; Pillai, P. P. Regulation of Interparticle Forces Reveals Controlled Aggregation in Charged Nanoparticles. *Chem. Mater.* **2016**, *28*, 2348-2355.

(15)   Rao, A.; Govind, S.; Roy, S.; Ajesh, T. R.; Devatha, G.; Pillai, P. P. Emergence of Selectivity in Inherently Nonselective Gold Nanoparticles through Preferential Breaking of Interparticle Interactions. ChemRxiv. **2018**, doi.org/10.26434/chemrxiv.7195817.v1

(16)   Tien, J.; Terfort, A.; Whitesides, G. M. Microfabrication through Electrostatic Self-Assembly. *Langmuir*, **1997**, *13*, 5349–5355.

(17)   Jana, N. R.; Peng, X. Single-Phase and Gram-Scale Routes toward Nearly Monodisperse Au and Other Noble Metal Nanocrystals. *J. Am. Chem. Soc.* **2003**, *125,* 14280–14281.

(18)   Pillai, P. P.; Huda, S.; Kowalczyk, B.; Grzybowski, B. A. Controlled PH Stability and Adjustable Cellular Uptake of Mixed- Charge Nanoparticles. *J. Am. Chem. Soc.* **2013**, *135*, 6392-6395.

(19)   Rao, A.; Roy, S.; Unnikrishnan, M.; Bhosale, S. S.; Devatha, G.; Pillai, P. P. Regulation of Interparticle Forces Reveals Controlled Aggregation in Charged Nanoparticles. *Chem. Mater.* **2016**, *28*, 2348-2355.

(20)   Kalsin, A. M.; Kowalczyk, B.; Smoukov, S. K.; Klajn, R.; Grzybowski, B. A. Ionic-like Behavior of Oppositely Charged Nanoparticles. *J. Am. Chem. Soc.* **2006**, *128*, 15046–15047.

(21)   Bishop, K. J. M.; Kowalczyk, B.; Grzybowski, B. A. Precipitation of Oppositely

Charged Nanoparticles by Dilution and / or Temperature Increase. *J. Phys. Chem. B.* **2009**, 113, 1413–1417.